

# Influence of Tool Deformations and Mounting Inaccuracies on 3D Surface Topology

A. Logins<sup>1</sup>, P. Rosado Castellano<sup>1</sup>, S. C. Gutiérrez Rubert<sup>1</sup>, R. Torres<sup>1</sup>, T. Torims<sup>2</sup>, F. Sergejev<sup>3</sup>

<sup>1</sup>Universitat Politècnica de València, Department of Mechanical and Materials Engineering, Valencia, Spain

<sup>2</sup>Riga Technical University, Department of Material Processing Technology, Riga, Latvia

<sup>3</sup>Tallinn University of Technology, Department of Materials Engineering, Tallinn, Estonia

## Abstract

In milling operations, tangential and normal cutting forces induce normal, tangential and axial elastic tool deformations. Tool mounting in the machine spindle may also contribute to kinematical errors. There is reason to believe that this phenomenon affects the milled surface formation and 3D surface topology parameters of final surface.

We performed simple, flat-end milling operations on C45 steel to compare results of surface total height measurements and prediction results done by using mathematical model developed by this article authors. Surface measurements were taken with an optical 3D surface topography evaluating device. Analysis identified significant tool deflections during the high-speed milling process. These combined with kinematical inaccuracies produce a complex tool movement that is basically responsible for the surface topology formation and 3D surface roughness parameter values. A similar approach could also be used to analyse more complex milling operations, such as those used in die and mould manufacturing.

## Keywords:

KEYWORDS: 3D surface topology, tool deflection, flat end milling

## 1 INTRODUCTION

Surface roughness is a means of defining the characteristics of mechanically machined surfaces. In recent years, most researchers in scientific fields have adopted 3D surface topology as a reference in process analysis. Surface topology provides a broader view of the machined surface quality. 3D surface topology is directly related to the 2D surface roughness measured in orthogonal planes. Topology measurements and analysis are important when undertaking complex machining operations, to ensure a high-quality machined surface. This technology is widely used to machine high-strength materials such as mould steels and to produce injection dies and moulds with a high surface quality [2, 3].

In metal cutting, several factors influence the final surface topology. Basic, general factors include machine cutting conditions that depend on the material, tool type and processing operation (rough or final machining). Changing these conditions affects the surface topology. In addition to these cutting conditions, there are other, independent factors:

- tool axis inclination;
- milling head inclination;
- tool deflection;
- tool runout or sharpening errors;
- chatter;
- etc.

Some factors, like tool inclination and sharpening errors, are constant during a complete tool revolution. Tool deflection and vibrations change over time and depend on the tool's rotational or immersion angle  $\lambda$ . Any combination of the above factors may affect the surface formation and probably also variously influence the surface formation process, by changing the cutting edge angular location, known as the immersion angle. Tool deflection and chatter are directly related to cutting forces. Cutting forces can be represented as a function of cutting conditions and material properties. The instant

cutting force is a variable which depends on the tool's angular rotation or immersion angle  $\lambda$  [1, 3, 12]. In this paper we discuss the theoretical model of surface formation, taking into account dependent and independent cutting factors. Our goal is to study and analyse the influence of tool forces, milling head alignment and tool sharpening errors and their combined interaction on topology and surface parameters. In this work we want to consider the surface topology formation with the tool's lower cutting edge.

## 2 STATE OF ART

Numerous authors have looked to develop a reliable cutting force prediction model, based on geometrical approaches. In the Cartesian coordinate system, the cutting force is a sum of cutting edge force projections of tangential, normal and axial forces, on a tool's local coordinate system [3, 5, 6, 8]. Some authors have developed models to predict surface formation taking into account tool chatter and runout parameters. In this case, they aim to predict topology on the laterally machined surface. They use tool chatter to simulate the surface topology, which is obtained by measuring tool displacement during the cutting process [4, 7, 10]. Only few of these authors inquire how these factors affect the surface performed by the lower cutting edge. The phenomenon of back cutting was considered in some additional research [1, 4, 5, 7]. Back cutting occurs when material is removed by the cutting edge of a tool part which is not involved in the instant cutting process. The residual surface profile after back cutting is determined by the phase difference and the magnitude of tool deflection [7].

M. Arizmedi [10] and Dae Kyun Baek [4] with their colleagues developed a simple approximation model to predict the surface roughness of laterally machined surface, based on the geometrical displacement and runout of the tool cutting edges. P. Franco [5] developed a surface prediction model for the face milling operation. He

uses a descriptive model to include tool sharpening error in the surface roughness prediction model.

Two types of factors influence the tool cutting edge trajectory – constant and instant. The tool's total inclination angle  $\theta_T$  consists of three components: the tool deflection angle  $\theta_{def}$ , which is an instant value and depends on the cutting force  $F_c$ ; the milling head inclination angle  $\theta_i$  which is a constant value and depends on the machine's geometrical errors (Figures 7 and 8); and the milling head and tool inclination angle, which is dependent on rotation. The cutting force  $F_c$  is an instant value and depends on material behaviour, uncut chip thickness,  $t_m$ , and axial cutting depth,  $a_p$ . The uncut chip thickness however is an instant value, and depends on feed and the cutter's immersion angle  $\lambda$ :

$$t_c = a_p * t_m = a_p * f * \sin(\lambda) \quad (1)$$

where  $f$  – feed per tooth,  $a_p$  – cutting axial depth.

**Milling head inclination** is the tool axis inclination angle relative to the plane of the tool path. It appears by milling head alignment inaccuracies. This inaccuracy is constant along the feed direction.

**Tool deflection** in cutting process is dependent of cutting forces. Tangential and normal cutting forces vary with cutter immersion angle  $\lambda$ . [8, 15] In the early studies of the milling process, the cutting force models were developed based on the nominal instantaneous uncut chip thickness without runout [8].

**Tool manufacturing errors**, including **tool sharpening errors** could generate tool runout errors, i.e. discrepancies between the theoretical axis and the tool's real rotation axis. These errors may influence cutting forces and cutters edge trajectory as well [9, 10, 14].

Comprehensive analysis of behaviour during the cutting process and its incidence on surface topology parameters requires consideration of all the factors involved in this process.

### 3 METHODOLOGY

Flat-end milling provides a good starting point from which to distinguish the machined surface topology created by each tool cutting edge. It is thus simpler to analyse milling head inclination, tool deflection and tool runout behaviour and their impact on surface topology parameters. Flat-end milling operations were performed with 2 flute cylindrical-end milling tools, under the following cutting conditions:

- Feed:  $f = 0.1$  mm/tooth
- Spindle speed:  $n = 4775$  rpm, equivalent to cutting speed  $V_c = 150$  mm/min
- Cutting depth:  $a_p = 0.3$ mm

The cutting procedures were performed using a rounded rectangular tool movement strategy to ensure straight tool movement in any feed direction. Figure 1 illustrates the areas (1. = South, 2. = West, 3. = North, 4. = East) where cutting was performed.

The material machined in the experiment was C45/ AISI 1045 carbon steel, widely used for injection mould production, where the machined surface quality has an important role in the final part.

KONDIA B500 CNC milling machine was used. Figure 1. illustrates the sample processing schematics and numbers related to the measurement order. A MITSUBISHI flat-end milling tool MS2MSD1000 with a cutting diameter (D) of 10mm was selected for the machining process (Figure 2). It is a tungsten carbide (WC) cutting tool with a MITSUBISHI UWC - TiAlN miracle coating. The tool has a secondary edge radial

relief angle ( $\sigma$ ) of 2°, a helix angle ( $\beta$ ) of 30° and 2 flutes.. Cutters edge point radius is too small to be measured with equipment available.

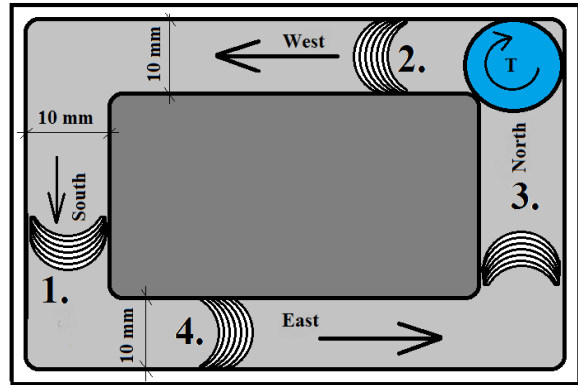


Figure 1: Cutting strategy of machined samples

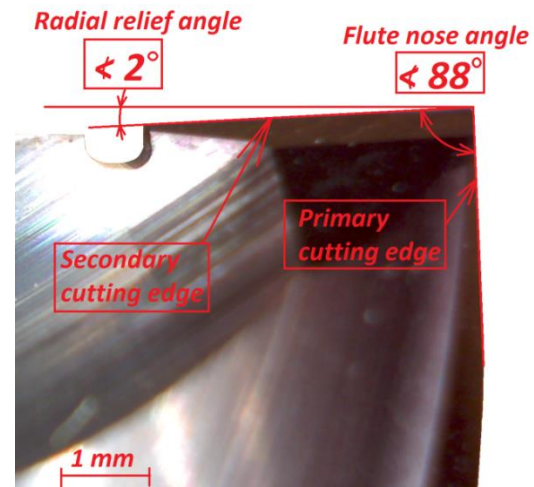


Figure 2: MITSUBISHI MS2MSD1000 cutting tool geometry

The 3D surface measurements were performed at Tallinn University of Technology, in the Faculty of Mechanical Engineering. The measurements were taken with a Bruker Contour GT3 optical measuring device. After measurement, the data was processed with MountainsMap Premium surface topology analysis software. The cutting topology is represented in Figure 4. Surface topology has been described by ISO 25178-2:2012 Geometrical Product Specification standard. It describes parameters  $S_z$  - Maximum height of scale limited surface.  $S_z$  expresses the sum of the maximum value of peak height,  $Z_p$ , and the maximum value of valley depth,  $Z_v$ , on the surface within the limited area [13]. Additional parameters widely used for surface height description are  $S_a$  – arithmetical mean height of the scale-limited surface and  $S_q$  – root mean square height of the scale-limited surface parameters [13].

Microscope photography and visual analysis of samples was carried out, to highlight the factors influencing surface formation in this cutting process.

To analyze cutting process, two different Finite Element Method (FEM) simulations were performed, to model cutting process simulation and analyze cutting force model. FEM simulation was performed taking in account all cutting tool geometrical parameters obtained from tool measurements and material properties from tool manufacturer (Figure 2.).

Whereas FEM software was used to analyze cutting force impact on tool deflection and determine tool rigidity coefficients. Tool deflection along Z axis causes tool

cutting edge displacement from its initial position. Realistic tool CAD model was made to obtain precise results of tool deflection (Figure 3.).

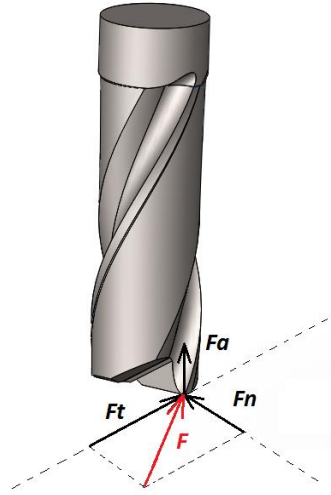


Figure 3: Cutting force interaction on flat end milling tool  
A mathematical model was then developed to calculate the cutting tool tip's angular movement and its deviation from the initial trajectory. The experimental results were analysed and compared with the mathematical model.

## 4 RESULTS

### 4.1 Visual analysis

Visual analysis of sample surface topology images and microscope photographs revealed marks on the material's surface that clearly shows us the tool movement direction. The surface pattern is dependent on a tool feed direction (Figure 4).

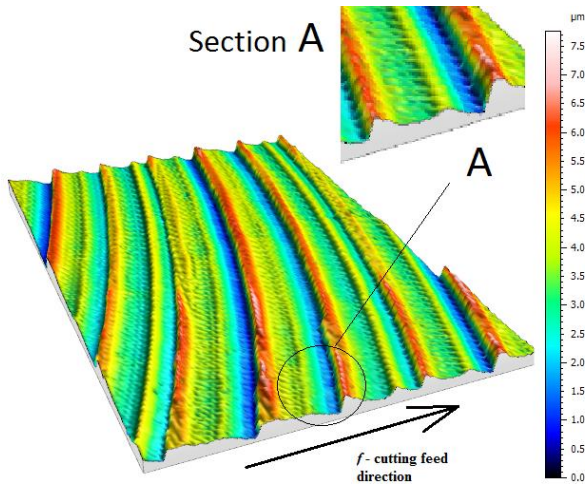


Figure 4: Surface topology measurements in area near to highest chip thickness.

More flat surface peak's slope decreases in the cutting feed direction. This slope results from the cutter's clearance in direction to the center. Distances between the highest peaks approximately coincide with defined cutting feed per tooth. Every repeated peak-valley pair is unique. Between them exists non-linear forms that are not constant in every step. Figure 4. Represent cutting marks on material surface left by the cutting edge. In left side of cut, accordingly to feed direction, we can observe the back cutting effect, marks indicated in figure 4. – Section A. These marks coincide with milling head inclination effect and occur in other samples accordingly with feed

direction. The same phenomenon is illustrated in the microscope image (Figure 5. –Section B).

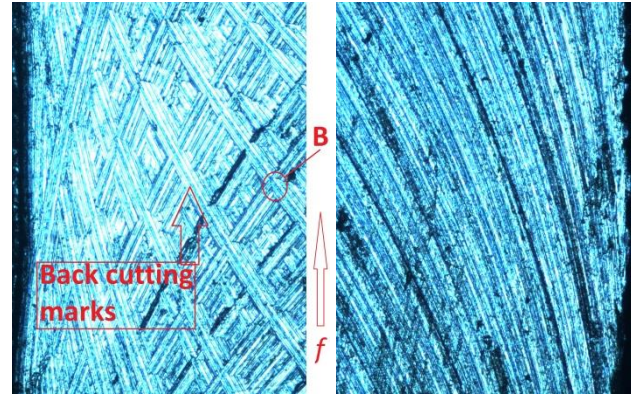


Figure 5: Surface topology microscope pictures – North direction sample's left and right region, according to feed direction.

### 4.2 Cutting force model development

The tangential  $F_t$ , normal  $F_n$  and axial force  $F_a$  cutting force model components can be determined by a general, well known model that uses three pressure coefficients  $K_t$ ,  $K_n$  and  $K_a$ . A simplified cutting force model can be used to determine the cutting pressure coefficients [6]:

$$F_t(\lambda) := K_t \cdot t_c(\lambda) \quad (2)$$

$$F_n(\lambda) := K_n \cdot (K_t \cdot t_c(\lambda)) \quad (3)$$

$$F_a(\lambda) := K_a \cdot (K_t \cdot t_c(\lambda)) \quad (4)$$

Where  $K_t$  is the cutting pressure from tangential force,  $K_n$  and  $K_a$  are cutting force coefficients as a function of  $K_t$  and  $t_c$  is the uncut chip cross section.

From the milling process simulation, we obtain cutting forces in global Cartesian coordinate system [6]. To determine cutting force coefficients from measurement or simulated data, it is necessary to express global cutting forces as a sum of force coefficients:

$$F_x(\lambda) := -F_t(\lambda) \cdot \cos(\lambda) - F_n(\lambda) \cdot \sin(\lambda) \quad (5)$$

$$F_y(\lambda) := F_t(\lambda) \cdot \sin(\lambda) - F_n(\lambda) \cdot \cos(\lambda) \quad (6)$$

$$F_z(\lambda) := F_a(\lambda) \cdot \sin(\lambda) \quad (7)$$

where  $\lambda$  – is tool immersion angle measured by the Y axis,  $F_n$ ,  $F_t$  and  $F_a$  – are normal, tangential and axial forces accordingly,  $F_x$ ,  $F_y$  and  $F_z$  are the cutting forces on the global coordinate system.

Substituting equations (2), (3) and (4) in (5), (6) and (7) and using a fitting method we can obtain the values of cutting coefficients:  $K_t = 2563 \text{ N/mm}^2$ ,  $K_n = 0.0089$  and  $K_a = 0.269$ . The plot of cutting forces (Figure 6) represents the behavior of cutting forces:

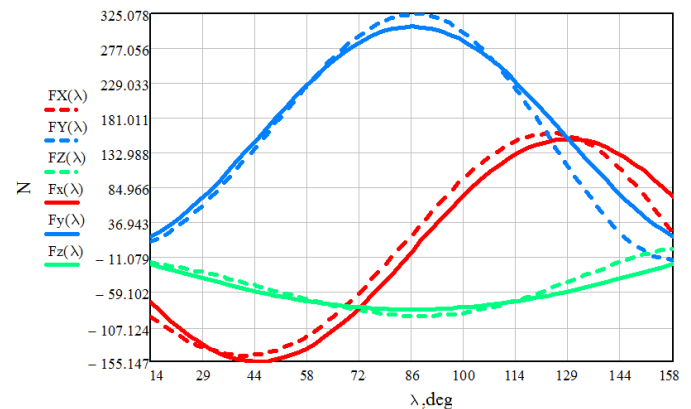


Figure 6: Plot of cutting forces  $F_x$ ,  $F_y$  and  $F_z$  along the tool immersion angle  $\lambda$ .

Discontinuous lines represent simulated cutting forces, but continuous line – with force model predicted cutting forces.

#### 4.3 Tool deflection model

To analyze tool cutting force influence on tool deflection along z axis, we developed a FEM simulation. In cutting process, there are working tangential ( $F_t$ ), normal ( $F_n$ ) and axial ( $F_a$ ) cutting forces against the tool cutting edge (Figure 3.). From simulation we collect the displacement data of the tool cutting edge. From data analysis we obtained 4 different material stiffness coefficients:

Deformation direction		Stiffness coefficient, N/mm
Tangential		$M_r = 8146.374$
Normal		$M_n = 11334.784$
Axial	Tangential component	$M_{z(t)} = 40150.968$
	Normal component	$M_{z(n)} = 57703.738$
	Axial component	$M_{z(a)} = 15885.716$

Table 1. Material C45 rigidity coefficients

where  $M_r$  – is Tool rigidity in normal force direction,  $M_t$  – is a tool rigidity in tangential force direction,  $M_{z(t)}$  – is a tool rigidity in axial direction by tangential force influence,  $M_{z(n)}$  - tool rigidity in axial direction by normal force influence,  $M_{z(a)}$  – is a tool rigidity in axial direction by axial force influence.

Tool deflection models accordingly to global machine coordinate system can be calculated by substituting rigidity coefficients into force model (Eq. 5, 6 and 7):

$$\delta X(F_x(\lambda)) = -F_t(\lambda) * \frac{1}{M_t} * \cos(\lambda) - F_n(\lambda) * \frac{1}{M_n} * \sin(\lambda) \quad (8)$$

$$\delta Y(F_y(\lambda)) = F_t(\lambda) * \frac{1}{M_t} * \sin(\lambda) - F_n(\lambda) * \frac{1}{M_n} * \cos(\lambda) \quad (9)$$

$$\delta Z(F(\lambda)) = \left( -F_t(\lambda) * \frac{1}{M_{z(t)}} \right) + \left( -F_n(\lambda) * \frac{1}{M_{z(n)}} \right) + \left( F_a(\lambda) * \frac{1}{M_{z(a)}} \right) \quad (10)$$

#### 4.4 Milling head inclination model

We used kinematical approaches to develop the geometrical model of how the tip of the cutting edge moves over the surface, where there is a constant milling head inclination. Figure 7. represents the tool circumference point translation (A and A''), caused by milling head inclination.

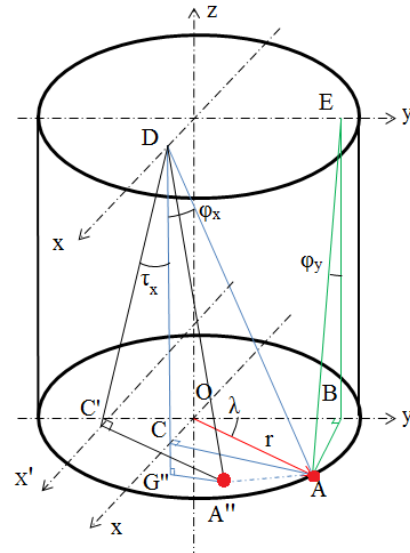
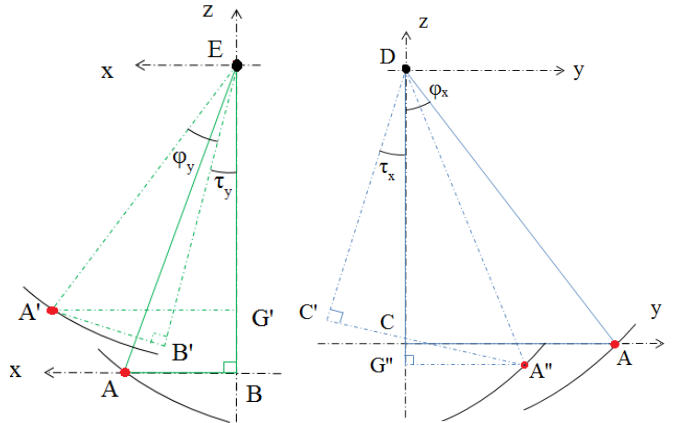


Figure 7: Tool circumference point translation

Angle  $\phi_x$  and  $\phi_y$  is internal tool triangle projection angle, that depends on tool length and immersion angle  $\lambda$ . Milling head inclination in y axis direction makes point A translation to point A''. We can project both points on XZ and YZ planes, similarly like to H. Jiang [9] proposed model, and thereby calculate the influence of milling head inclination in both coordinates X and Y.

Therefore, we explain it with two projections (Figure 8. a and b). We consider that points D and E belong to axis X and Y. Feed direction is on X axis. Tool cutting edge trajectory instant displacement can be calculated accordingly with tool length, diameter and immersion angle. In this calculation  $BE = CD =$  tool height.



a) Inclination on X axis

b) Inclination on Y axis

Figure 8. Milling head inclination projections in global coordinate system

Milling head inclination on X axis makes the tool cutting edge trajectory displaced from A to A'. Displacement on XZ plane has two coordinates. Z coordinate displacement is equal to G'B. To differential between initial and displaced Z coordinate, we calculate hypotenuse of triangle ABE:

$$AE = A'E = \sqrt{(r * \sin(\lambda))^2 + (BE)^2} \quad (14)$$

This hypotenuse is equal to displaced triangle A'G'E hypotenuse A'E. From this triangle we can calculate cathetus, adding up the tool internal triangle projection angle  $\phi_y$  with the inclination angle on X axis  $\tau_y$ :

$$A'G' = \sqrt{(r * \sin(\lambda))^2 + (H)^2} * \sin(\phi_y + \tau_y) \quad (15)$$

Differential of z value or G'B can be calculated with the following equation:

$$\delta z_x(\lambda) = BE - \sqrt{(A'E)^2 - (A'G')^2} \quad (16)$$

Similarly, the same point displacement is projected on YZ plane, where tool deflection and inclination is considered on Y axis (Figure 8.b). Initial triangle ACD, has a direct relation with deformed triangle A''C'D. The deformed triangle is caused by milling head inclination angle  $\tau_x$ . By the same manner like previously, we assume to calculate hypotenuse and cathetus of displaced internal triangle projection on YZ plane:

$$AD = A''D = \sqrt{(r * \cos(\lambda))^2 + (CD)^2} \quad (11)$$

$$A''G'' = \sqrt{(r * \cos(\lambda))^2 + (H)^2} * \sin(\varphi_x + \tau_x) \quad (12)$$

Differential of z value or G''C can be calculated with the following equation:

$$\delta z_y(\lambda) = CD - \sqrt{(A''D)^2 - (A''G'')^2} \quad (13)$$

where  $\delta z_x(\lambda)$  and  $\delta z_y(\lambda)$  – z height differential from inclination at x and Y axis accordingly, r – cutter radius,  $\lambda$  – tool cutting edge immersion angle, H – tool height,  $\tau_x$  and  $\tau_y$  – milling head inclination angle in X and Y axis direction respectively,  $\varphi_x(\lambda)$  and  $\varphi_y(\lambda)$  – tool length and radius defined internal triangle projection angle.  $\delta z_x(\lambda)$ ,  $\delta z_y(\lambda)$  and total variation on z direction,  $\delta z(\lambda)$ , from two kinematical projections has been plotted in Figure 10.

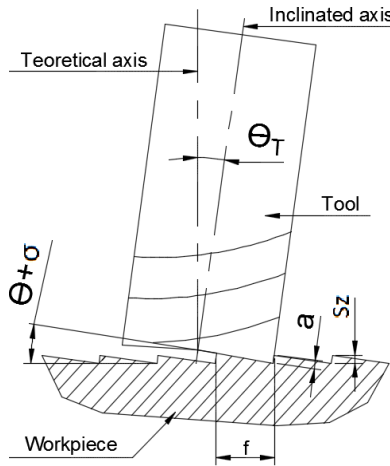


Figure 9. Total tool inclination angle  $\theta_T$

In the cutting process is acting other parameter, affected by tool geometry. With every rotation, tool cutting edges with complimentary angle of  $88^\circ$  perform minimal surface topology height. Secondary cutting edge has radial relief angle  $\sigma = 2^\circ$ , therefore this minimum height can be calculated with equation developed in previous research [16], subtracting milling head inclination angle  $\theta$ :

$$\delta z_T(\lambda) = \frac{t(\lambda) * \tan(\theta + \sigma)}{1 + \tan(\theta + \sigma) * \tan(\theta)} \quad (17)$$

Where,  $\theta$  – milling head inclination angle without tool deflection angle,  $\sigma$  – secondary cutting edge radial relief angle.

In Figure 9. Sz – surface total height, f – feed per tooth,  $\theta + \alpha$  – milling head inclination angle and secondary cutting edge radial relief angle sum,  $\theta_T$  – milling head inclination angle, a – triangle side length.

Total variation on z direction,  $\delta z(\lambda)$ , is calculated as a sum of each component:

$$\delta z(\lambda) = \delta z_x(\lambda) + \delta z_y(\lambda) + \delta Z(F(\lambda)) + \delta z_T(\lambda) \quad (18)$$

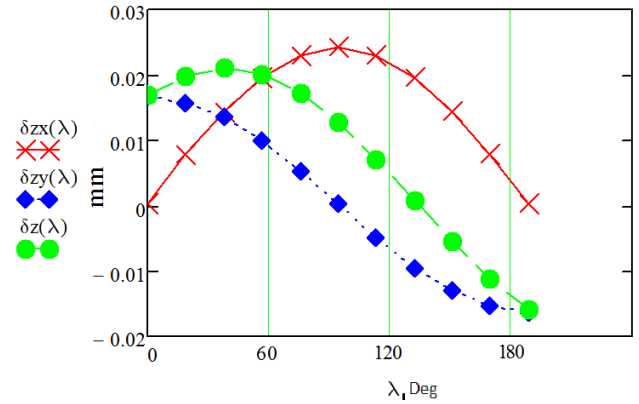


Figure 10: Plot of differential of Z coordinate value depending on immersion angle.

#### 4.5 Predicted surface analysis

When all input data was determined we plotted a mathematical model to analyze tool cutting edge point movement trajectory and its deviations.

We compare mathematical results with measured results. The estimated model presents tool point deviation in whole tool overlap. Measurement regions were rectangular zones of 1,25mm x 1,7mm. Realistic surface height values were obtained only from within these areas. Table 2 represents mathematically estimated values from tool tip point rotation. To calculate tool trajectory the following variables were used: tool length H = 34.8mm, axial runout  $\rho = 0.001$  mm, Milling head inclination around x axis  $\tau_x = 0.376^\circ$ , around y axis  $\tau_y = 0.547^\circ$ . Including the tool axial runout variable, we observed deviation for every cutting edge from the initial tool tip trajectory. The trajectory deviation remains at the same level.

A comparison of mathematically obtained values and average measurement results (Table 2.) shows that in the mathematical approach, the same surface formation behaviour appears, i.e. the South direction, the average difference is greater than in the North direction. The same was observed in the East and West directions. The difference between measured and mathematically obtained values presents an error of 19% in West-East directions, and 28% in South-North direction. Therefore, in all directions, the predicted topology is from 12% to 16% lower. Measured values are always higher than those simulated ones. They represent the worst cutting situation, although this situation is not always reflected in the actual cutting process. As the amplitude of values are  $\mu\text{m}$  then every small change in process generates big difference in results. That can affect the result, and relatively the error of 12 – 28% is acceptable.

Feed direction	Sa value measured, $\mu\text{m}$	Sz value measured, $\mu\text{m}$	Sz value simulated, $\mu\text{m}$	Difference error between measured and predicted, $\mu\text{m}$ , %	Difference error between directions, %	
					Measured	Predicted
1. South	1.01733	10.60445	8.6750839	1.2228	24%	28%
	1.16082	9.19131		12%		
3. North	1.14825	8.29217	6.7668536	1.224066		

	0.89045	8.46029		15%		
2. West	1.12516	8.0833	7.063988	1.31224066	16%	19%
	1.16229	7.89854		16%		
4. East	1.00001	9.33774	8.3779497	1.31164		
	1.09779	10.04144		14%		

Table 2. Measured and predicted surface topology parameters analysis

## 5 CONCLUSIONS

Microscope images of surface samples confirm the influence of milling head inclination and tool deflection on surface formation. It is not easy to predict the trajectory of the tip of the tool's cutting edge as it travels over the material workpiece. In all samples we obtained back-cutting marks from the secondary cutting edge owing to the machine milling head inclination error. In all samples this behaviour was repeated compared with the machine coordinate system. As the cutting edge tip angle reaches 180°, tool deflection is minimal as the uncut chip thickness tends towards 0. The tool returns to its initial position, maintaining its initial inclination. The secondary cutting edge becomes closer to material and leaves back cutting marks on the surface. This reduces the total height of the surface topology. Similarly this phenomenon can be observed when cutting starts, where only the milling head and tool inclination should be considered.

The developed mathematical model represents tool cutting edge movement. This movement includes high tool deformations along the tool's z axis and cutting edge deviations from the initial trajectory. In the area corresponding to the measured topology width, this model represents the surface's greatest height differences, but considering the area of full tool overlap, it reflects surface geometrical errors like machined surface inclination, waviness, etc.

The mathematically obtained results show that in all end-milling operations, milling head inclination error and tool initial geometry have the highest influence on the surface formation created by the lower cutting edge. Tool deflection is the next important factor.

Axial tool runout changes the tool tip's depth compared with the initial point, but not the height deviation amplitude per revolution. Therefore, every secondary cutting edge step may affect the surface height formation – different slope and shallower valleys. Topology measurement images confirm this behaviour. High tool runout may affect uncut chip thickness and subsequently cutting forces. This can have a minor influence on tool deflection and surface topology height.

The discrepancies between measurements and predicted model represent the influence of other effects working in the cutting process that are not considered in this article. These may be tool inclination error, chatter and material elasticity behaviour, among others. The next step will be to update this mathematical model with these missing factors, to obtain a full mathematical description of the cutting edge trajectory and surface topology height.

## 6 REFERENCES

- J.W. Sutherland, T.S. Babin, "The geometry of surfaces generated by the bottom of an end mill", *Sensors and Controls for Mechanics* 1988, ASME PED, Vol. 33, pp. 53-62;
- Schulz H., Moriwaki T., „High – Speed Machining”, *Ann. of the CIRP*, 1992, t. 41, nr 2, pp.637 –642 p.;
- S. Engin, Y. Altintas, Mechanics and dynamics of general milling cutters. Part I: helical end mills, *International Journal of Machine Tools & Manufacture* 41 (2001) 2195–2212;
- D.K. Baek, T.J. Ko, H.S. Kim, "Optimization of feed rate in a face milling operation using a surface roughness model", *International Journal of Machine Tools & Manufacture* 41 (2001) pp. 451-462;
- P. Franco, M. Estrems, F. Faura, "Influence of radial and axial runouts on surface roughness in face milling with round insert cutting tools", *International Journal of Machine Tools & Manufacture* 44 (2004) pp. 1555-1565;
- E. Budak, Analytical models for high performance milling. Part I: Cutting forces, structural deformations and tolerance integrity, *International Journal of Machine Tools & Manufacture* 46 (2006) 1478–1488;
- S. H. Ryu, D. K. Choi, C. N. Chu, Roughness and texture generation on end milled surfaces, *International Journal of Machine Tools & Manufacture* 46 (2006) 404–412;
- W. Min, Z. Wei-hong, T. Gang, Q. Guo-hua, New Cutting Force Modeling Approach for Flat End Mill, *Chinese Journal of Aeronautics* 20(2007) 282-288;
- H. Jiang, X. Long, G. Meng, Study of the Correlation Between Surface Generation and Cutting Vibrations in Peripheral Milling, *Journal of materials processing technology* 208 (2008) 229–238;
- M. Arizmendi, F.J. Campa, J. Fernandez, L.N. Lopez de Lacalle, A. Gil, E. Bilbao, F. Veiga, A. Lamikiz, "Model for surface topology prediction in peripheral milling considering tool vibration", *CIRP Annals - Manufacturing Technology* 58 (2009) pp. 93-96;
- M. Wan, W.Zhang, J. Dang, Y. Yang, novel cutting force modelling method for cylindrical end mill, *Applied Mathematical Modelling* 34 (2010) 823–836;
- J.W. Dang, W. Zhang, Y. Yang M. Wan, "Cutting force modelling for flat end milling including bottom edge cutting effect", *International Journal of Machine Tools & Manufacture* 50 (2010) pp. 986-997;
- International Organization for Standardisation., ISO 25178-2:2012 - Geometrical product specifications (GPS) -- Surface texture: Areal -- Part 2: Terms, definitions and surface texture parameters, ICS: 17.040.20, 47 p.;
- B. Denkena, M. Kruger, D. Bachrathy, G. Stepan, Model based reconstruction of milled surface topology from measured cutting forces, *International Journal of Machine Tools & Manufacture* 54–55 (2012) 25–33;
- Z. Fu, W. Yang, X. Wang, J. Leopold, Analytical Modelling of Milling Forces for Helical End Milling Based on a Predictive Machining Theory, 15th CIRP Conference on Modelling of Machining Operations, *Procedia CIRP* 31 (2015) 258 – 263;
- Logins, P. Rosado Castellano, T. Torims, S. C. Gutiérrez Rubert, F. Sergejev, Experimental analysis

of how the inclination error of flat-end milling tools  
influences 3D surface topology parameters, 11th  
International DAAAM Baltic Conference

"INDUSTRIAL ENGINEERING" - 20th-22nd April  
2016, Tallinn, Estonia;